Communications in Physics, Vol. 33, No. 4 (2023), pp. 457-470
DOI: https://doi.org/10.15625/0868-3166/18643

Research on the synthesis of TiO_2 and SiO_2 nanoparticles for anti-bacterial exterior and interior wall paints

Khoi Nguyen Dang[1,2], **Van Cuong Bui**[1], **Hai Khoa Le**[1], **Pham Thi Lan**[1,2†], **Dai Lam Tran**[1]

[1] *Institute for Tropical Technology, Vietnam Academy of Science and Technology, 18 Hoang Quoc Viet, 10000 Hanoi, Vietnam*

[2] *Graduate University of Science and Technology, Vietnam Academy of Science and Technology, 18 Hoang Quoc Viet, 10000 Hanoi, Vietnam*

E-mail: †ptlan@itt.vast.vn

Received 18 April 2023; *Accepted for publication 15 July 2023*; *Published 13 December 2023*

Abstract. *TiO_2 has strong photocatalytic activity, which can oxidize and decompose impurities on surfaces and in the air. Therefore, TiO_2 is used as an additive in the self-cleaning coating and paint industries. In this work, SiO_2 is used in the TiO_2/SiO_2 mixture as the nucleus to homogenize the dispersion components. TiO_2 and SiO_2 nanoparticles are synthesized by the sol-gel method combined with ultrasound that suits the size range of 10-30 nm. The nano mixture is added to two paint samples, denoted as EWT (exterior wall paint) and IWT (interior wall paint) to replace antibacterial agents in paint formulations. In the results, two paint samples showed antibacterial capability in accordance with ASTM D2574-06 for antibacterial paints.*

Keywords: antibacterial activity; coating; nanoparticles; titanium dioxide; silica dioxide.
Classification numbers: 61.46.Df; 81.15.Rs.

1. Introduction

In recent decades, nanotechnology and nanomaterials have made significant breakthroughs, contributing to solving many global challenges that humanity faces in fields such as healthcare, energy, and the environment. Nanostructured materials have a strong appeal due to their size reduction from the macroscopic scale to the nanoscale, resulting in significant changes in electronic conductivity, optical absorption, chemical reactivity, and mechanical properties. Materials with sizes ranging from 100 nm down to the atomic level can exhibit distinct or enhanced properties compared to their larger counterparts.

In the field of coatings and paint, nanotechnology and nanomaterials have been widely applied in various sectors, including defense, oil and gas, automotive, electronics, and civil applications. Due to the physical and chemical properties related to size effects, many types of coatings incorporate nano-sized particles, showing superior effectiveness. Modern techniques such as the sol-gel method have been successfully employed to fabricate nanostructured coatings with superior properties compared to conventional organic coatings [1–3].

However, organic coatings often do not provide long-term protection due to their brittle structure and degradation when exposed to environmental factors. Furthermore, the small pores created within the coating during curing through the evaporation of organic solvents create favorable conditions for the diffusion of corrosive agents such as water molecules and Cl^- ions through the coating to the substrate. Functional coatings are defined as coatings that effectively perform a specific property of the substrate, such as self-cleaning, corrosion resistance, water repellency, self-healing, solar reflectivity, weatherability, waterproofing, and more. Such coatings possess superior properties compared to conventional organic coatings and fall into the category of "green coatings" because they either do not use or use very few environmentally harmful solvents and raw materials [4].

The beneficial use of nanoparticles brings many advantages and opportunities to the paint and coating industry. The addition of nanoparticles in coatings improves many properties of the coating system and creates multi-purpose coatings. For example, some nanoparticles with the functions of heat reflection, UV absorption, weather resistance, self-cleaning, and anti-fouling such as SiO_2, TiO_2, $BaSO_4$, Fe_2O_3, ZnO...These coatings are suitable for weapons storage, petroleum tanks and civil uses (mirrors, self-cleaning windows, brick, etc.).

A photocatalyst is a chemical reaction induced by light, specifically using UV radiation with wavelengths ranging from 100 to 400 nm, directly applied to catalyst materials such as metal plates like TiO_2, ZnO or MnO_2 [5, 6]. Among them, TiO_2 is considered the most effective. TiO_2 possesses strong photocatalytic properties, oxidizing and decomposing contaminants on surfaces and in the air. The process of UV radiation on these metal plates generates free radicals (OH^-) and (O_2^{-1}), which exhibit strong oxidative capabilities [5]. These free radicals can oxidize volatile organic compounds (VOCs) in the air, as well as bacteria and mold, converting them into CO_2 and water [5]. Due to these remarkable properties, TiO_2 is utilized as an additive in the production of self-cleaning coatings for industries such as paints and coatings [7]. TiO_2 can also be synthesized in nanoparticles form to enhance the efficiency of the photocatalytic process and accelerate the degradation of organic compounds. Additionally, other antibacterial components can be combined with TiO_2 to increase the antibacterial properties of the mixture [8].

This antibacterial mechanism is environmentally friendly and avoids the development of drug resistance as well as genetic mutations in disease-causing microorganisms. The small size of nanoparticles reduces the recombination process of electrons and holes while enhancing the photocatalytic performance of the material. Additionally, nano-TiO_2 particles have the ability to self-clean and remove dirt as the coating surface becomes more hydrophilic after the photocatalytic oxidation process (formation of •OH groups on the coating surface) [9, 10].

However, like many other types of nano, when added to the paint system, TiO_2 is susceptible to agglomeration, thereby reducing the antibacterial ability of the material. SiO_2 is used in the TiO_2/SiO_2 mixture as a matrix to homogenize the dispersed components of TiO_2/SiO_2 and other nano-materials when added to the composite [11–13]. The silica matrix reduces aggregation and enhances the antibacterial activity of nano-sized components in the coating mixture [11–13]. Some studies have incorporated silver nanoparticles (Ag NPs) into the TiO_2/SiO_2 system, significantly enhancing its antibacterial properties [14, 15]. In other research, reduced graphene oxide (RGO) has also been added to the TiO_2/SiO_2 system using tetraethoxysilane (TEOS) [16]. The results demonstrate a significant improvement in antibacterial performance. Thus, the addition of TiO_2 and SiO_2 nanoparticles improved the advantages of the two components and the properties of the paint film, such as the fact that nano TiO_2 has an antibacterial effect and nano SiO_2 has the effect of increasing the washability and UV resistance of the paint film, while minimizing the agglomeration of nanoparticles in the paint film. In Vietnam, the commonly used antibacterial and antifungal paint systems involve the addition of organic biocides, which have different concentrations depending on the specific biocidal agents used [17, 18]. When these components are added to the coating system, they effectively resist mold and fungi. However, these antibacterial agents, when dispersed into the environment, can have potential impacts on human health. Moreover, these agents may not persist in the material for long, resulting in reduced antibacterial and antifungal efficacy over time. By incorporating inorganic antibacterial agents with photocatalytic properties such as TiO_2 and SiO_2, the drawbacks of using chemical biocides in paint systems can be addressed effectively. Therefore, in this study, we will research and manufacture two types of interior wall paint and exterior wall paint composed of TiO_2 and SiO_2 nanoparticles. Nanoparticles will be researched and manufactured separately using the sol-gel method, then added simultaneously to two paint formulas, from which the antibacterial abilities of the two paints will be researched.

2. Materials and methods

2.1. Chemicals

Materials for the synthesis of TiO_2 and SiO_2 nanoparticles include, titanium isopropoxide (TTIP) at 97%, tetraetyl orthosilicat (TEOS) at 99.0%, poly ethylene glycol (PEG) at 400 and amoniac at 25% were provided by Sigma-Aldrich, whereas, ethanol at 99.7% and methanol at 99.5%, were obtained from Xilong Ltd. (China).

Ingredients for making paint formula, include Strodex TH-100 phosphate ester, Drew plus T4507, Natrosol 250 HBR, pHlex 110 and Aquaflow NHS300 were purchased from Ashland, USA; DIRTSHIELD 12 and Orotan 1124 were purchased from Dow, USA; FOAMASTER MO NDW NC was obtained BASF, Germany. Texanol Ester Alcohol was obtained from Eastman, USA; TiO_2 was obtained from Dupont, Taipei.

All chemicals were used without further purification.

2.2. Synthesis of TiO_2 and SiO_2 nanoparticles

Synthesis of TiO_2 nanoparticles

Mix 50 ml of TTIP with 50 ml of ethanol to obtain a precursor solution, referred to as solution 1. Dissolve H_2O in 50 ml of ethanol to form solution 2. Prepare solution 3, the reaction medium, by dissolving 100 ml of PEG 400 in 400 ml of ethanol. Simultaneously add solution 1 and solution 2 to solution 3 in a reaction vessel. The reaction vessel is placed in an ultrasonic bath operating at a frequency of 37 kHz and a temperature of 80°C, while being stirred at 350 rpm. Allow the reaction to proceed for 3 hours. After the completion of solutions 1 and 2, continue the ultrasonication process for an additional 15 hours. Ethanol is added during the reaction to maintain the volume of the reaction vessel. Cease ethanol addition and continue heating, ultrasonication, and stirring to remove ethanol from the reaction vessel and collect the product.

Table 1. Experimental conditions of precursors in TiO_2 nanoparticles synthesis.

No.	Samples	TTIP (g)	H_2O (g)	PEG
1	T1	4.0	1.0	100
2	T2	8.0	2.0	100
3	T3	12.0	3.0	100
4	T4	16.0	4.0	100

Synthesis of SiO_2 nanoparticles

Mix 35 ml of TEOS with 50 ml of ethanol to obtain a precursor solution, referred to as solution 1. Dissolve H_2O in 50 ml of ethanol to form solution 2. Prepare solution 3, the reaction medium, by dissolving 100 ml of PEG 400 in 400 ml of ethanol. Add NH_3 until the pH reaches approximately 13. Simultaneously add solution 1 and solution 2 to solution 3 in a reaction vessel. The reaction vessel is placed in an ultrasonic bath operating at a frequency of 37 kHz and a temperature of 80°C, while being stirred at 350 rpm. Allow the reaction to proceed for 4 hours. After the completion of solutions 1 and 2, continue the ultrasonication process for an additional 15 hours. During the reaction, add ethanol and NH_3 as needed to maintain the reaction environment. Cease ethanol addition and continue heating, ultrasonication, and stirring to remove ethanol from the reaction vessel and collect the product.

Table 2. Experimental conditions of precursors in SiO_2 nanoparticle synthesis.

No.	Samples	TEOS (g)	H_2O (g)	NH_3
1	S1	1.0	0.5	20
2	S2	2.0	1.0	20
3	S3	4.0	2.0	20
4	S4	6.0	3.0	20

2.3. Fabrication of antibacterial paints containing nano TiO_2 and nano SiO_2

Two types of antibacterial paints (denoted as EWT and IWT) containing nano mixtures of TiO_2 and SiO_2 are researched and manufactured with detailed ingredients listed in Table 3. TiO_2 and SiO_2 nanoparticle mixture was made in liquid form, then directly added to the paint formula to shorten the fabrication time and minimize the clumping of nanoparticles Paint samples were prepared by stirring with a speed of 600 rpm/minute for 30 minutes until a homogeneous mixture was obtained.

2.4. Characterisation

A feld emission scanning electron microscope (FE-SEM, HITACHI S-4800) and a transmission electron microscope (TEM), JEOL JEM-1010 were used to examine the morphology of TiO_2 and the SiO_2. Zeta potential analyses were done using an Otsuka Electronics DLS/Zeta SZ100 (Horiba, Japan).

Table 3. Composition of EWT and IWT paints fomulations.

No.	Material	Percent (%)	Weight, gram	Note
	Formulation of an EWT paint sample			
No.	**Material**	**Percent (%)**	**Weight, gram**	**Note**
1	DIRTSHIELD 12	50.00%	500	Binder (Resin)
2	FOAMASTER MO NDW NC	1.00%	10	De-foamer
3	Strodex TH-100 phosphate ester	0.50%	5	Surfactant
4	Orotan 1124	0.50%	5	Dispersant
5	Drew plus T4507	0.50%	5	Foam Control Agent
6	Texanol Ester Alcohol	1.00%	10	Coalescent
7	TiO_2	15.00%	150	Pigment
8	SiO_2 nanoparticle sol	6.50%	65	In this study
9	TiO_2 nanoparticle sol	2.00%	20	In this study
10	Natrosol 250 HBR	0.40%	4	Thickener
11	pHlex 110	0.20%	2	pH Neutralizing Agent
12	Aquaflow NHS300	2.00%	20	Rheology modifier
13	Water	20.400%	204	Solvent
	Total	**100.00%**	**1000**	
	Formulation of an IWT paint sample			
No.	**Material**	**Percent (%)**	**Weight (gram)**	**Note**
1	DIRTSHIELD 12	50.00%	500	Binder (Resin) Acrylic Polymer
2	FOAMASTER MO NDW NC	1.00%	10	De-foamer
3	Strodex TH-100 phosphate ester	0.50%	5	Surfactant
4	Orotan 1124	0.50%	5	Dispersant
5	Drew plus T4507	0.50%	5	Foam Control Agent
6	Texanol Ester Alcohol	1.00%	10	Coalescent
7	TiO_2	15.00%	150	Pigment
8	SiO_2 nanoparticle sol	6.50%	65	In this study
9	TiO_2 nanoparticle sol	3.50%	35	In this study
10	Natrosol 250 HBR	0.40%	4	Thickener
11	pHlex 110	0.20%	2	pH Neutralizing Agent
12	Aquaflow NHS300	2.00%	20	Rheology modifier
13	Water	18.900%	189	Solvent
	Total	**100.00%**	**1000**	

2.5. Antibacterial tests

The antimicrobial properties of the paints are evaluated against the gram-negative bacterium *Pseudomonas aeruginosa* ACTT 10145, following the standard ASTM D2574-06 method.

3. Results and Discussion

3.1. The influence of synthesis conditions on the size of TiO_2 nanoparticles

The effect of synthesis conditions on the particle size of TiO_2 was presented in Table 4. To investigate the effect of synthesis conditions on the particle size, the samples were analyzed and evaluated by the DLS analysis method.

The DLS analysis results indicate that all four samples have average particle sizes smaller than 25 nm. However, the zeta potential of sample T4 suggests that it is unstable (ranging from ±10 to ±30 mV) (Table 3, Fig. 1 and Fig. 2), while samples T1, T2 and T3 exhibit moderate stability.

Table 4. DLS results of TiO_2 samples.

No.	Samples	particle size (nm)	zeta potential (mV)	
1	T1	9.5	-37.7	
2	T2	11.2	-35.2	
3	T3	13.8	-32.4	
4	T4	19.4	-29.9	Image of T3 sample

The particle size of TiO_2 increases with increasing TTIP concentration, and the zeta potential gradually shifts towards the unstable region, indicating a propensity for aggregation and the formation of larger aggregates. Among the three samples (T1, T2 and T3), sample T3 has the highest expected TiO_2 concentration and is therefore chosen for further research.

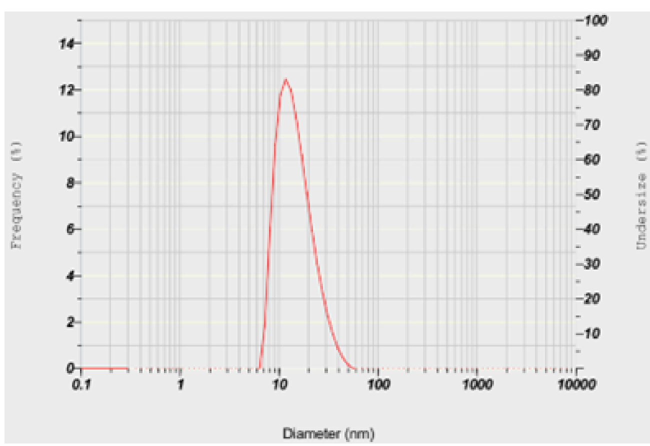

Fig. 1. DLS analysis of T3 sample.

The SEM analysis results indicate that the TiO_2 particle size is in the range of 50-60 nm (Fig. 3). The particles tend to agglomerate, forming clusters, and exhibit uneven distribution in the

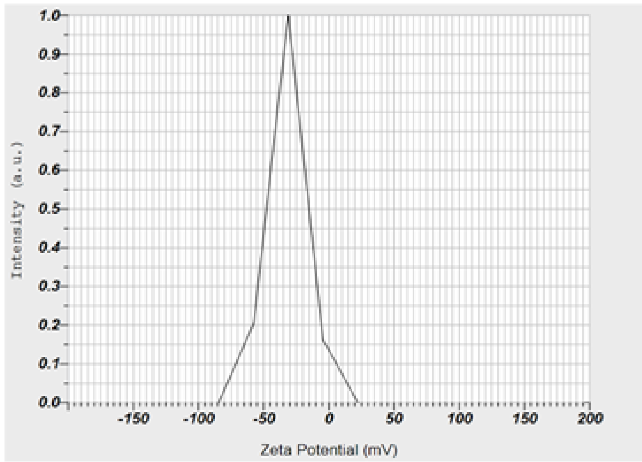

Fig. 2. Zeta potential analysis of T3 sample.

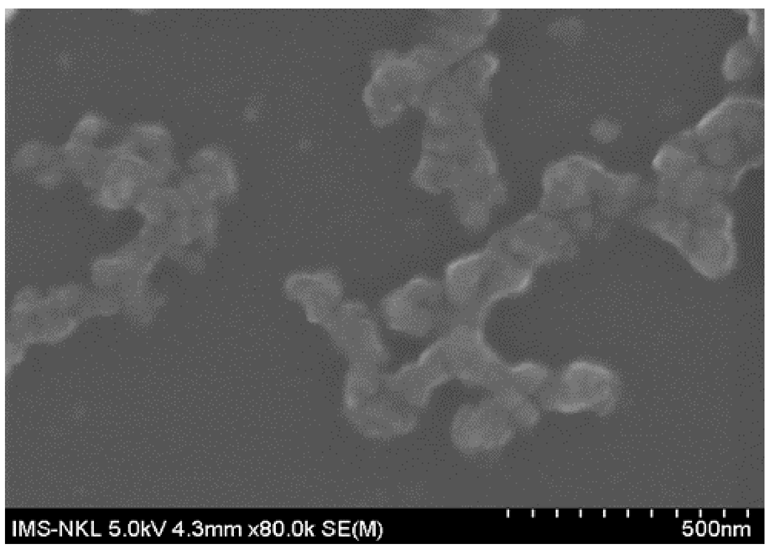

Fig. 3. SEM analysis of T3 sample.

dispersion medium. Therefore, the transmission electron microscopy (TEM) method is employed to provide a more detailed assessment of the analyzed sample (Fig. 4).

The TEM analysis results reveal that the TiO_2 nanoparticles have achieved a sub-nanometer size within the range of 10-30 nm. The nanoparticles appear to be well-dispersed, although their distribution on the analysis substrate is not uniform. This non-uniformity can be attributed to the influence of coating agents on the dispersion process of the nanoparticles in the appropriate dispersing medium (water).

The FTIR spectrum of T3 was obtained as shown in Fig. 5. The appearance of a broad band at approximately 3300 - 3350 cm^{-1} was assigned to the characteristic vibrations of the OH group

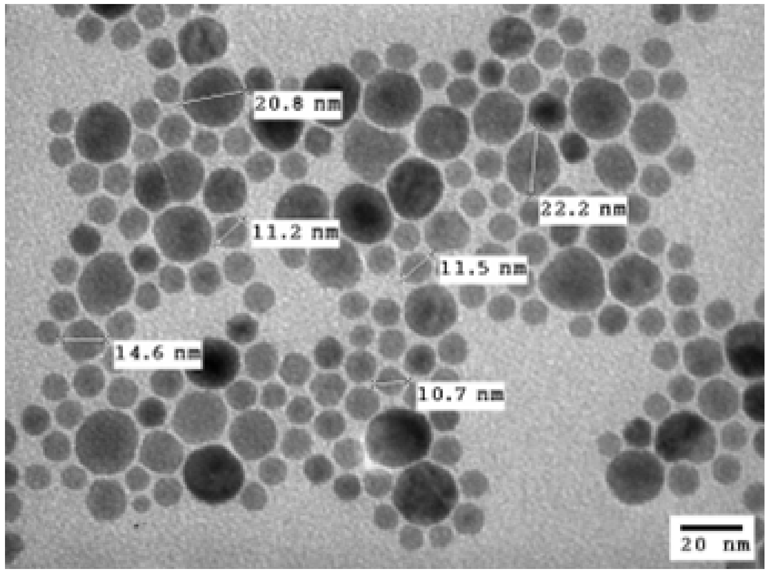

Fig. 4. TEM analysis of T3 sample.

of nano TiO_2. The peak at 3000-2800 cm^{-1} of the polymer alkyl group. This spectrum also shows characteristic peaks at 1650, 1400-1300 cm^{-1} which are consistent with the stretching groups of Ti-OH and C-H (also Ti-O), respectively. Besides, peaks at 1072.96 cm^{-1} corresponding to C-O valence vibration showed the bonding interaction between the coating and nano TiO_2 [19–21].

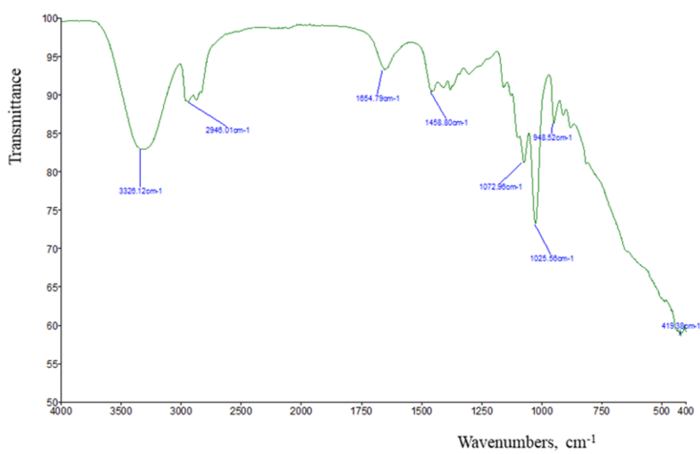

Fig. 5. FTIR analysis of T3 sample.

The FTIR results indicate the influence of the coating agent on the particles. The formation of bond bridges between polymer compounds and TiO_2 particles explains the interference phenomenon when analyzing the TEM images mentioned above.

3.2. The influence of synthesis conditions on the size of SiO_2 nanoparticles

Effect of TEOS/H_2O ratio on the particle size was investigated (Table 5).

Table 5. DLS results of SiO_2 samples.

No.	Sample	particle size (nm)	Zeta potential (mV)	
1	S1	250.1	-53.4	
2	S2	292.5	-48.2	
3	S3	331.7	-29.6	
4	S4	406.2	-21.2	Image of S2 sample.

The DLS analysis results indicate that all four samples have relatively large average particle sizes (above 250 nm). However, the zeta potential of samples S3 and S4 suggests that they are unstable (ranging from ±10 to ±30 mV), while samples S1 and S2 exhibit good stability. The nano-SiO_2 particle size increases rapidly with increasing TEOS concentration, and the zeta potential gradually shifts towards the unstable region, indicating a higher propensity for aggregation and particle formation. Between the two samples, S1 and S2, sample S2 has a higher expected concentration of nano SiO_2 and is therefore selected for further research and studies.

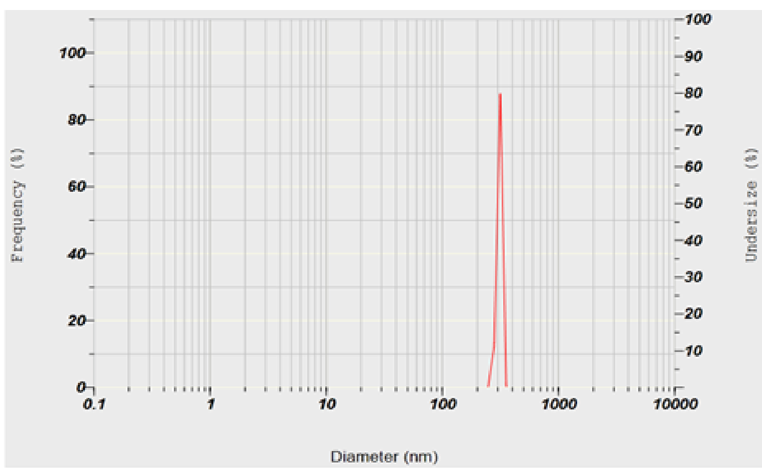

Fig. 6. DLS analysis of S2 sample.

The SEM analysis results reveal that the SiO_2 particles have a size range of 50–80 nm (Fig. 8). The particles are unevenly distributed and tend to partially agglomerate, which can impact the DLS measurement results.

The TEM analysis results show that the SiO_2 particles have achieved a size range of 10-30 nm and are evenly distributed in the dispersion medium (Fig. 9). Upon observing the TEM images,

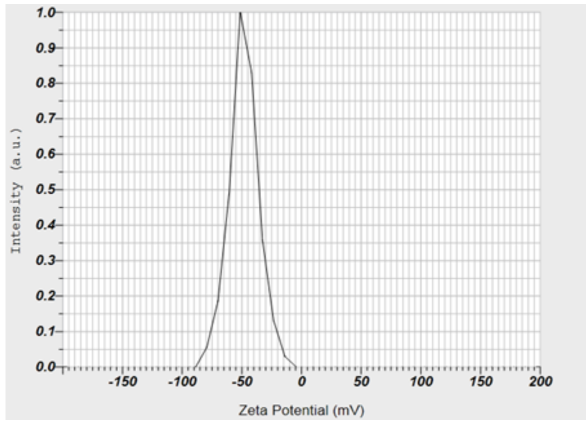

Fig. 7. Zeta potential of S2 sample.

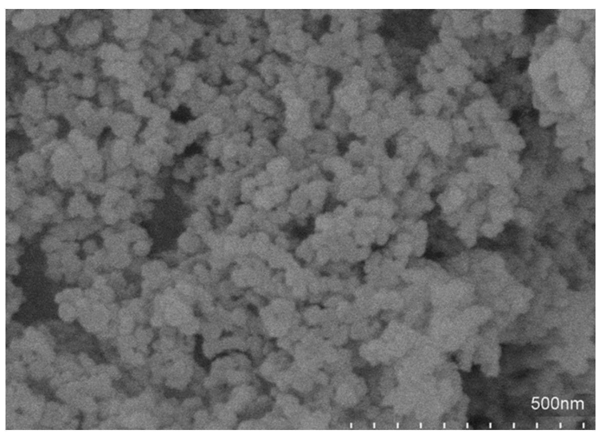

Fig. 8. SEM analysis of S2 sample.

it is evident that the SiO_2 nanoparticles tend to cluster, resulting in larger aggregates with sizes ranging from 40-50 nm. This phenomenon can be attributed to several factors: The formation of larger crystalline networks among SiO_2 nanoparticles with lower energy levels. The attractive forces between Si-O and Si-Si bonds are stronger than the bonding forces between the polymer and the nanoparticles. The presence of a large amount of coating agents that do not form strong bonds with the nanoparticles. These factors contribute to the clustering of SiO_2 nanoparticles and the formation of larger aggregates.

The chemical bonding of silica groups was investigated using FTIR spectroscopy, as shown in Fig. 10. In the FTIR spectrum at 1094,97 cm^{-1} and 455,71 cm^{-1} correspond to asymmetric valence vibrations and deformation vibrations of the Si-O-Si group. The peak at 798.99 cm^{-1} characterizes the Si-OH symmetric valence vibration of nano SiO_2 [22–24].

The FTIR results showed that SiO_2 particles tend to form similar particles with a network formation energy level lower than the energy level of particles coated with polymer. It confirmed

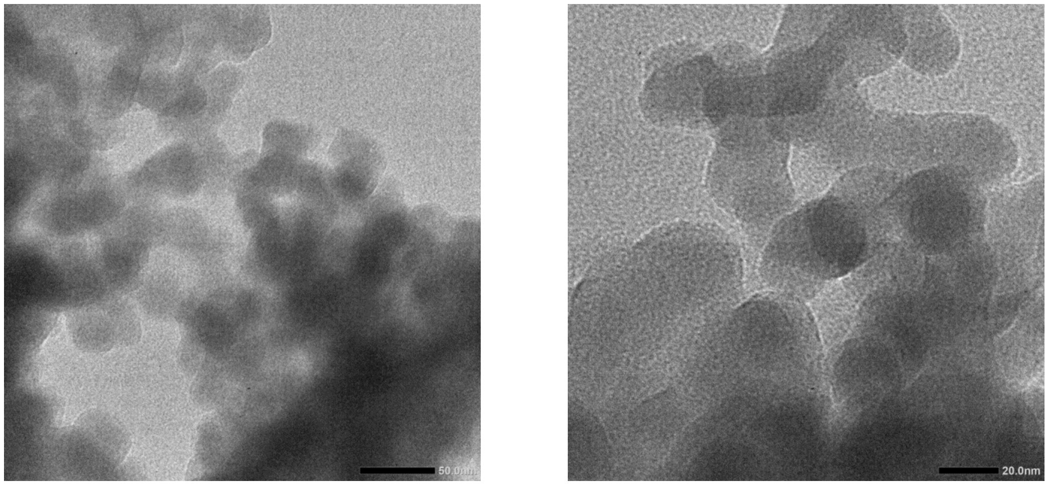

Fig. 9. TEM analysis of S2 sample.

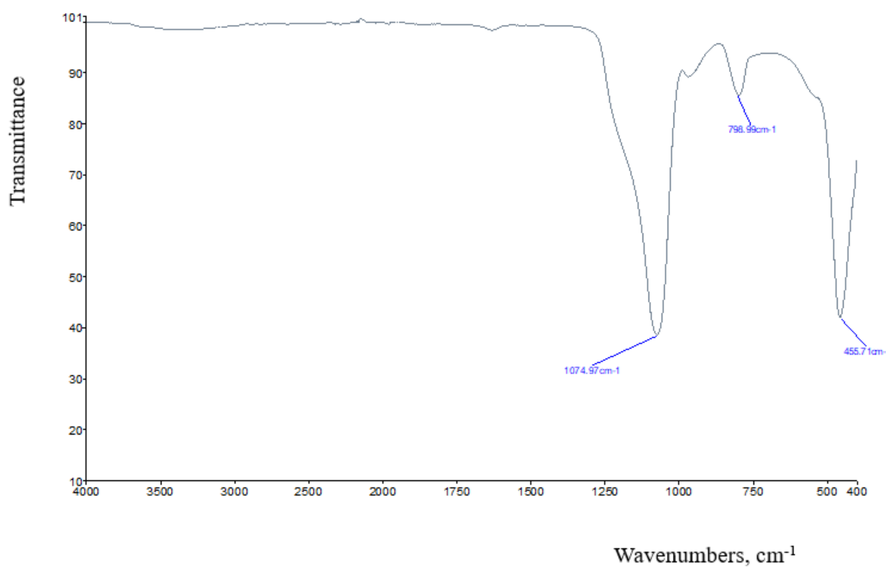

Fig. 10. FTIR analysis of S2 sample.

that the polymer compounds added during the synthesis process help stabilize the particles formed at a predetermined size.

3.3. Results of anti-bacterial activity of paints

The two paint lines based on the nano TiO_2-SiO_2 in tetraethoxysilane are referred to as EXT and INT. The antimicrobial efficacy results are presented in Table 6 and Table 7, and compared to the standard level set by the ASTM D2574-06 method.

The strain *Pseudomonas aeruginosa* is a gram-negative microorganism commonly found in soil environments and has the ability to spread in the air [25]. The experiment was conducted at two different levels of microbial quantity, which were 0.1 mL and 1 mL of bacterial solution at a concentration of 10^9 CFU/mL. The procedures were carried out following the ASTM D2574-06 standard to assess the paint-destructive capability of the bacterial strain. Generally, in a paint sample without antibacterial additives, bacterial growth will quickly occur, causing the paint to deteriorate, emitting odor gas, and significantly reducing the paint's viscosity. In samples of paint with antibacterial additives, this phenomenon will not occur or will occur very slowly [26].

Table 6. Analysis results of paint samples tested with 1 ml of bacterial solution with a bacterial density of 10^9 CFU/ml.

	3 days	***5 days***	***7 days***	***9 days***
Sample	*number of CFU*	*number of CFU*	*number of CFU*	*number of CFU*
EWT paint	2	0	0	0
Report according to ASTM-D2574-06 template	Bacterial infection (1 to 9 CFU)	No-bacterial ifnection	No-bacterial ifnection	No-bacterial ifnection
IWT paint	0	0	0	0
Report according to ASTM-D2574-06 template	No-bacterial ifnection	No-bacterial ifnection	No-bacterial ifnection	No-bacterial ifnection

Table 7. Analysis results of paint samples tested with 1 ml of bacterial solution with a bacterial density of 10^9 CFU/ml.

Sample	***3 days***	***5 days***	***7 days***	***9 days***
	number of CFU	*number of CFU*	*number of CFU*	*number of CFU*
EWT paint	21	3	1	0
Report according to ASTM-D2574-06 template	Light-bacterial infection (10 to 99 CFU)	Bacterial infection (1 to 9 CFU)	Bacterial infection (1 to 9 CFU)	No-bacterial ifnection
IWT paint	3	1	0	0
Report according to ASTM-D2574-06 template	Bacterial infection (1 to 9 CFU)	Bacterial infection (1 to 9 CFU)	No-bacterial ifnection	No-bacterial ifnection

The results of the antibacterial evaluation of the paint after the testing period show that the control sample (without the addition of the nano TiO_2-SiO_2) quickly exhibited signs of being damaged by the bacterial strain. Gas produced in the control paint sample had a foul odor, and there was a thin layer of separated, frothy solution on the surface of the test paint, leading to a reduction in paint viscosity. In contrast, no such phenomena were observed in the paint samples with the addition of the nano system.

The results of testing bacterial density (CFU/mL) in experimental paint samples indicate that both paint lines demonstrate excellent antimicrobial properties when compared to the levels set by the ASTM D2574-06 standard. With the addition of 0.1 mL of bacterial suspension to the paint, there is almost no bacterial growth observed within the paint (Table 6). When the amount of bacterial suspension is increased to 1 mL, there is initial mild contamination observed in the paints. However, after 7 to 9 days, there is no evidence of bacterial growth in either paint line (CFU/mL = 0) (Table 7). The results indicate that the nano TiO_2-SiO_2 system effectively works when added to paint, causing a clear antibacterial effect at the selected concentration.

Nano TiO_2-SiO_2, has been studied for its antimicrobial properties. The antimicrobial activity of nano TiO_2-SiO_2 is primarily attributed to its photocatalytic properties, specifically when exposed to ultraviolet (UV) light. The energy from the UV light activates the TiO_2 nanoparticles, creating electron-hole pairs. These electron-hole pairs generate highly reactive oxygen species (ROS), such as hydroxyl radicals (•OH) and superoxide radicals ($O_2{}^{\bullet -}$) [27]. ROS can interact with the lipid bilayer of the bacterial cell membrane, causing lipid peroxidation and disrupting the integrity of the membrane. ROS can also damage proteins and DNA inside the bacterial cells [28].

4. Conclusion

In this study, TiO_2 and SiO_2 nanoparticles are investigated for synthesis by sol-gel method combined with ultrasound. The results show that the average size of TiO_2 nanoparticles is 14 nm with a zeta potential of -34 mV, while SiO_2 nanoparticles has an average size of 20 nm with a zeta potential of -38 mV. TiO_2 and SiO_2 nanoparticles are replaced with antibacterial agents in two paint samples. The paint samples show antibacterial ability in accordance with ASTM D2574-06 for antibacterial paints.

Acknowledgement

This work was supported by the Vietnam Academy of Science and Technology under grant number TĐVLTT.01/21-23.

Conflict of interest

The authors have no conflict of interest to declare.

References

[1] J. Sahoo, S. Sarkhel, N. Mukherjee, A. Jaiswal. *Nanomaterial-Based Antimicrobial Coating for Biomedical Implants: New Age Solution for Biofilm-Associated Infections*, ACS Omega **7** (2022) 45962.

[2] S. M. Imani, L. Ladouceur, T. Marshall, R. Maclachlan, L. Soleymani, T. F. Didar, *Antimicrobial Nanomaterials and Coatings: Current Mechanisms and Future Perspectives to Control the Spread of Viruses Including SARS-CoV-2*, ACS Nano **14** (2020) 12341.

[3] D. Bokov, A. T. Jalil, S. Chupradit, W. Suksatan, M. J. Ansari, I. H. Shewael *et al.*, *Nanomaterial by Sol-Gel method: synthesis and application*, Adv. Mater. Sci. Eng. (2021) 5102014.

[4] W. J. van Ooij, D. Zhu, M. Stacy, A. Seth, T. Mugada, J. Gandhi, *et al.*, *Corrosion protection properties of organofunctional silanes -An Overview*, Tsinghua Sci. Tech. **10** (2005) 639.

[5] J. N. U. Krishnan, B. J. S. Chandra, J. S. Ajish, *Effective tri-metallic TiO_2 supported catalyst for hydrocarbon production from carbon dioxide*, J. Indian Chem. Soc. **100** (2023) 100859.

[6] T. A. Gokhale, V. V. Phatake, B. M. Bhanage, *MnO_2 nanostructures as sustainable catalysts for selectivity tuning and syntheses of amine coupling products with bio-derived glycerol*, Mol. Catal. **533** (2022) 112771.

[7] N. T. Padmanabhan, H. John , *Titanium dioxide based self-cleaning smart surfaces: A short review*, J. Environ. Chem. Eng. **8** (2020) 104211.

[8] B. Pant, M. Park, SJ. Park, *Recent Advances in TiO_2 films prepared by Sol-Gel methods for photocatalytic degradation of organic pollutants and antibacterial activities*, Coatings **9** (2019) 10.

[9] J. Arun, S. Nachiappan, G. Rangarajan, R. P. Alagappan, K. P. Gopinath and E. Lichtfouse, *Synthesis and application of titanium dioxide photocatalysis for energy, decontamination and viral disinfection: a review*, Environ. Chem. Lett. **21** (2023) 339.

[10] Nasikhudin, M. Diantoro, A. Kusumaatmaja and K. Triyana. *Study on Photocatalytic Properties of TiO_2 Nanoparticle in various pH condition*, J. Phys. Conf. Ser. **1011** (2018) 012069.

[11] A. Rosales, K. Esquivel, *SiO_2@TiO_2 composite synthesis and its hydrophobic applications: a review*, Catalysts **10** (2020) 171.

[12] B. K. Tudu, A. Sinhamahapatra and A. Kumar, *Surface modification of cotton fabric using TiO_2 Nanoparticles for self-cleaning, oil–water separation, antistain, anti-water absorption, and antibacterial properties*, *ACS Omega* **5** (2020) 7850.

[13] V. Kumaravel, K. M. Nair, S. Mathew, J. Bartlett, J. E. Kennedy, H. G. Manning et al., *Antimicrobial TiO_2 nanocomposite coatings for surfaces, dental and orthopaedic implants*, Chem. Eng. J. **416** (2021) 129071.

[14] X. Yan and P. Pan, *Preparation of Silver Antibacterial Agents with Different Forms and Their Effects on the Properties of Water-Based Primer on Tilia europaea Surface*, Coatings **11** (2021) 1066.

[15] T. Bakalova, L. Svobodová, P. Rosická, K. Borůvková, L. Voleský, P. Louda, *The application potential of SiO_2, TiO_2 or Ag nanoparticles as fillers in machining process fluids*, J. Clean. Prod. **142** (2017) 2237.

[16] G. Yi, B. Xing, H. Zeng, X. Wang, C. Zhang, J. Cao, L. Chen. O*ne-Step Synthesis of Hierarchical Micro-Mesoporous SiO_2 /Reduced Graphene Oxide Nanocomposites for Adsorption of Aqueous Cr(VI)*, J. Nanomater. **2017** (2017) 6286549.

[17] T. T. Le, T. V. Nguyen, T. A. Nguyen, T. T. H. Nguyen, H. Thai, D. L. Tran *et al.*, *Thermal, mechanical and antibacterial properties of water-based acrylic polymer/SiO_2-Ag nanocomposite coating*, Mater. Chem. Phys. **232** (2019) 362.

[18] N. T. Vuong, N. T. Anh, D. P. Hung, M. V. Phuc, N. A. Hiep, D. M Thanh and N. T. Huu, *Effect of rutile titania dioxide nanoparticles on the mechanical property, thermal stability, weathering resistance and antibacterial property of styrene acrylic polyurethane coating*, Adv. Nat. Sci: Nanosci. Nanotechnol. **7** (2016) 045015.

[19] G. Devanand, S. Ramasamy, B. Ramakrishnan, J. Kumar, *Folate targeted PEGylated titanium dioxide nanoparticles as a nanocarrier for targeted paclitaxel drug delivery*, Adv. Powder Technol. **24** (2013) 947.

[20] N. Sanaz, R. Hamid, F. Mohammad, S. Mhammad, M. Morteza, *Mortality response of folate receptor-activated, PEG-functionalized TiO_2 nanoparticles for doxorubicin loading with and without ultraviolet irradiation*, Ceram. Int. **40** (2014) 5481.

[21] D. Nadica, M. Abazovic, M. Comor, D. Dramicanin, S. Jovanovic, M. Jovan, *Photoluminescence of Anatasese and Rutile TiO_2 Particles*, J. Phys. Chem. B **110** (2006) 25366.

[22] N. T. Chinh, N. T. T. Trang, V. Q. Manh, T. Hoang, *Total nanosilica composite and EVA/silica nanocomposite materials have supporting uses EVAgMA compatible*, Vietnam J. Chem. **50** (2012) 96 (in Vietnamese).

[23] J. Chruściel and L. Ślusarski, *Synthesis of nano silica by the sol-gel method and its activity toward polymers*, Mater. Sci. **21** (2003) 461.

[24] K. R. Martin, *The chemistry of silica and its potential health benefits*, J. Nutr. Health. Aging **11** (2007) 94.

[25] Y. M. Briand and C Baysse, *The pyocins of Pseudomonas aeruginosa*, Biochimie **84** (2002) 499.

[26] H.R Ravikumar, SS Rao, CS Karigar. *Biodegradation of paints: a current status*, Indian J. Sci. Technol. **5** (2012) 1977.

[27] U. Mahanta, A. S. Deshpande and M. Khandelwal, *TiO_2 decorated SiO_2 nanoparticles as efficient antibacterial materials: enhanced activity under low power UV light*, ChemistrySelect **8** (2023) e202203724.

[28] H. V. Acker, T. Coenye. *The role of reactive oxygen species in antibiotic-mediated killing of bacteria*, Trends Microbio. **25** (2017) 456.